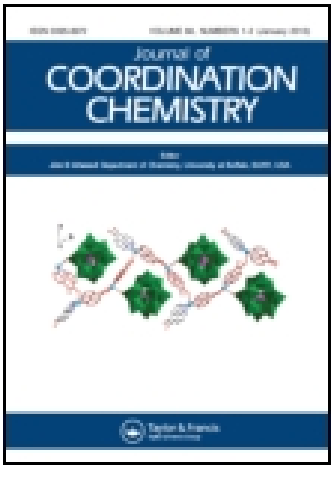

Journal of Coordination Chemistry
Publication details, including instructions for authors and subscription information:
http://www.tandfonline.com/loi/gcoo20

New homobimetallic organotin(IV) dithiocarbamates as potent antileishmanial agents

Sher Ali[a], Zia-ur-Rehman[a], Muneeb-ur-Rehman[b], Imran Khan[c], Syed Niaz Ali Shah[a], Rana Faryad Ali[a], Afzal Shah[a], Amin Badshah[a], Kamran Akbar[a] & Francine Bélanger-Gariepy[d]

[a] Department of Chemistry, Quaid-i-Azam University, Islamabad, Pakistan

[b] Department of Physics, Islamia College University, Peshawar, Pakistan

[c] Department of Biotechnology, Quaid-i-Azam University, Islamabad, Pakistan

[d] Département de Chimie, Université de Montréal, Montreal, Canada

Accepted author version posted online: 01 Sep 2014.Published online: 23 Sep 2014.

To cite this article: Sher Ali, Zia-ur-Rehman, Muneeb-ur-Rehman, Imran Khan, Syed Niaz Ali Shah, Rana Faryad Ali, Afzal Shah, Amin Badshah, Kamran Akbar & Francine Bélanger-Gariepy (2014) New homobimetallic organotin(IV) dithiocarbamates as potent antileishmanial agents, Journal of Coordination Chemistry, 67:20, 3414-3430, DOI: 10.1080/00958972.2014.960406

To link to this article: http://dx.doi.org/10.1080/00958972.2014.960406

Journal of Coordination Chemistry, 2014
Vol. 67, No. 20, 3414–3430, http://dx.doi.org/10.1080/00958972.2014.960406

New homobimetallic organotin(IV) dithiocarbamates as potent antileishmanial agents

SHER ALI†, ZIA-UR-REHMAN*†, MUNEEB-UR-REHMAN‡, IMRAN KHAN§, SYED NIAZ ALI SHAH†, RANA FARYAD ALI†, AFZAL SHAH†, AMIN BADSHAH†, KAMRAN AKBAR† and FRANCINE BÉLANGER-GARIEPY¶

†Department of Chemistry, Quaid-i-Azam University, Islamabad, Pakistan
‡Department of Physics, Islamia College University, Peshawar, Pakistan
§Department of Biotechnology, Quaid-i-Azam University, Islamabad, Pakistan
¶Département de Chimie, Université de Montréal, Montreal, Canada

(*Received 2 May 2014; accepted 24 July 2014*)

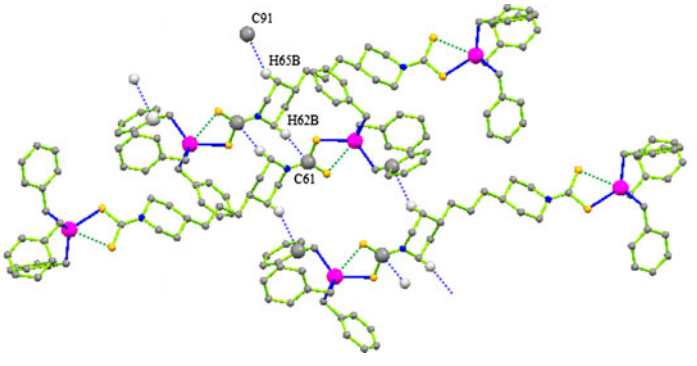

Four new homobimetallic organotin(IV) dithiocarbamates have been synthesized and characterized by different analytical techniques. These compounds have pronounced antileishmanial and antimicrobial activities.

In the present study, di- and triorganotin(IV) dithiocarbamates, $(n\text{-}Bu_2SnCl)_2L$ (**1**), $(Ph_2SnCl)_2L$ (**2**), $(Ph_3Sn)_2L$ (**3**), and $(Bz_3Sn)_2L$ (**4**), have been synthesized, where L is 4,4-trimethylenedipiperidine-1-carbodithioate. The coordination mode of the ligand to Sn, structural confirmation and geometry assignment around Sn(IV), in solid and solution forms, were made using FT-IR, multinuclear NMR (^1H and ^{13}C), and X-ray single crystal analysis. The latter technique confirms anisobidentate mode of chelation of the ligand with Sn, in **1–4**, with distorted trigonal bipyramidal or square pyramidal geometry. Complexes **1–4** present supramolecular structures mediated by different C···H and Cl···H intermolecular interactions. These complexes maintain five-coordination even in solution, except for **4**. The antileishmanial activity of all complexes are well above the standard drug, especially $(Bz_3Sn)_2L$. The Docking studies suggest that high antileishmanial action of $(Bz_3Sn)_2L$ is due to its lowest binding energy with enzyme trypanothione synthetase. The antileishmanial activity of the complexes is promising enough that they may be used for antileishmanial treatment after further investigations.

*Corresponding author. Email: zrehman@qau.edu.pk

Keywords: Homobimetallic; Organotin; Antileishmanial; Supramolecular; Dithiocarbamate

1. Introduction

Tropical diseases constitute a leading health issue and a big challenge for drug development. These diseases affect about one-third of the total world population and cause 2 million deaths annually, mostly in the poorest areas of the globe. Among these leishmaniasis is an ailment with extensive morbidity and mortality. Currently, 12 million people worldwide with 2 million new cases per year suffer from this disease. Moreover, leishmaniases are widespread in 88 countries, including 72 developing countries [1]. In order to fight this lethal and quickly diffusing disease, several drugs have been used including pentavalent antimonials with sodium stibogluconate (pentostam) and meglumine antimoniate (glucantine). However, these drugs suffer from negative side effects and chemoresistance developed by the parasite [2]. So there is an urgent need for drugs with more efficacy and limited or no side effects.

Several efforts have been made in this context. Zinc sulfate was tested clinically against cutaneous leishmaniasis with very promising cure rates (>96.0%) using oral doses of 10 mg kg^{-1} for 45 days [3]. A DNA Pt(II)-based intercalator showed complete growth inhibition of *Leishmania donovani amastigotes* at 1 mM concentration. This complex has the ability to do simultaneous DNA intercalation and enzyme active site binding. The most probable reason is the similarity between the tumor cells and the kinetoplastid parasites [4–6]. This idea was further supported by another effort in which new metallointercalators were found with promising antileishmanial activity [7]. Fricker *et al.* proposed that gold(III), palladium(II), and rhenium(V) cyclometallated complexes block active site (thiol group) of cysteine proteases which ultimately lead to the parasite's death [8]. Salma *et al.* reported significant *in vitro* antileishmanial activity of germatranyl substituted organotin(IV) carboxylates and germatranyl and silicon-incorporated diorganotin derivatives against promastigotes of leishmania donovani and promastigotes of *Leishmania major* [9, 10].

In order to enhance the drug efficacy and to minimize the associated side effects, it is vital to understand the structure–activity relationship. Docking is one of the tools that is used to elucidate the most energetically favorable binding pose of a drug to its receptor [11]. Enzymes such as Trypanothione Synthetase (TryS) have been validated genetically and biochemically as a drug target in Leishmania and other trypanosomatids [12]. For Leishmania, TryS is bifunctional possessing both synthetase and amidase activities. The enzyme catalyzes the biosynthesis of trypanothione in an ATP-dependent reaction and also hydrolyzes dithiol [13]. TryS can be a potential target since it is a single copy gene in human parasites, and inhibition of the enzyme will not only lead to alteration in polyamine levels but also in depletion of substrate for trypanothione reductase via synthesis of thiols, thus disturbing redox homeostasis of the parasite [14].

Based on our previous findings [15, 16], we herein report four new homobimetallic organotin(IV) dithiocarbamates, and their antileishmanial activity. Moreover, we preformed molecular docking analysis of our synthesized drugs with crystallographic structure of TryS from Leishmania major. The goal was to correlate our experimental antileishmanial results with the most energetically favorable binding pose of drugs with TryS and to look for their inhibition pathways towards TryS of Leishmania major. According to the best of our knowledge, this will be the first antileishmanial report for organotin(IV) dithiocarbamates.

2. Results and discussion

2.1. *Spectroscopic characterization*

FT-IR bands were assigned to their respective functional groups by comparing the FT-IR spectra of the complexes with the precursors. New absorptions at 350–370 cm^{-1} and 420–480 cm^{-1} can be assigned to the Sn–S and Sn–C stretches, respectively [17]. In chlorodiorganotin(IV) derivatives (**1** and **2**), a peak associated with (Sn–Cl) was observed at 303–310 cm^{-1} which indicates the substitution of a single chloride of the diorganotin salt during the reaction. In the FT-IR study of organotin(IV) dithiocarbamates, two regions are of particular interest, the 1450–1550 cm^{-1} and 950–1050 cm^{-1} regions that are associated with ν(N–CSS) and ν(S–C), respectively. The complexes gave the ν(N–CSS) stretch at 1460–1510 cm^{-1}. These values are between the range reported for C=N double bond (1650–1690 cm^{-1}) and C–N single bond (1250–1350 cm^{-1}), and thus show C–N partial double bond character [18]. Moreover, ν(N–CSS) stretching vibration of the complexes is higher than the ligand, showing increase in C–N partial double bond character upon complexation [19]. For chlorodiorganotin(IV) derivatives, the ν(N–CSS) band is higher than triorganotin(IV) complexes due to the presence of chloro, which can withdraw electron density, and as a result positive charge increases on nitrogen. According to Bonati and Ugo [20], the peak at 950–1050 cm^{-1} is due to C–S stretch. A single symmetrical peak in this region is an indication of bidentate coordination whereas splitting of the peak shows monodentate coordination. The complexes presented a single peak in this region and thus point to bidentate coordination.

The proton NMR spectra of **1–4** were recorded in $CDCl_3$. The intensity, multiplicity patterns, and the chemical shifts were used to identify different nonequivalent protons. The expected molecular composition of the compound is in agreement with the total number of protons calculated from the integration curve. The [^{119}Sn, ^{1}H] coupling value gives information about the coordination of Sn in solution. For **4**, the observed value is 49 Hz that according to Lockhart's equation, $\theta = 0.0161\ [^2J]^2 - 1.32\ [^2J] + 133.4$, corresponds to CSnC angle of 107°. Thus, the Sn in **4** is four-coordinate in solution.

The peak due to CSS at 213.0 ppm shifted upfield by 18 ppm upon complexation. The upfield shift may be due to an increase in the electron density on 1,1-dithioate carbon due to the mobilization of nitrogen lone pair of NCSS towards CSS moiety. The observed ^{13}C chemical shift due to different organic groups attached to Sn was at comparable positions to other similar compounds [21]. The ^{1}J [^{119}Sn,^{13}C] coupling constant value and the calculated corresponding θ value from Lockhart's equation ($^{1}J = 10.7\theta - 778$) can be used to determine the coordination number of Sn [22]. The observed values for **1**, **2**, and **3** were 558 Hz (125°), 578 Hz (127°), and 600.7 Hz (129°), which are the typical values for five-coordinate Sn; however, the value 302 Hz corresponding to an angle of 103° for **4** match well with four-coordinate Sn. The appearance of a peak at chemical shift value of 142.7 ppm which is for *ipso*-C confirm five-coordinate Sn in the triphenyl derivative [23]. Thus, **1–3** maintained their solid-state coordination in solution. This fact can be explained on the basis of electron withdrawing nature of Sn attached phenyl and Cl groups, strengthening Sn–S bond.

2.2. *X-ray single crystal analysis*

In **1** and **2**, both tins of the homobimetallic complex are five coordinate, surrounded by two organic groups, a chloride, and two sulfurs from the ligand (figures 1 and 2, table 1). The

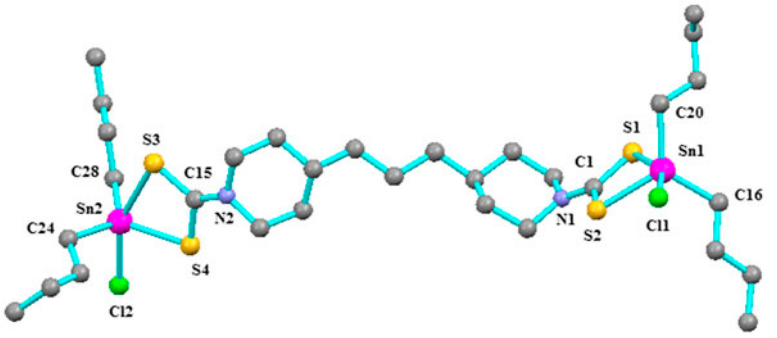

Figure 1. Molecular structure of **1**.

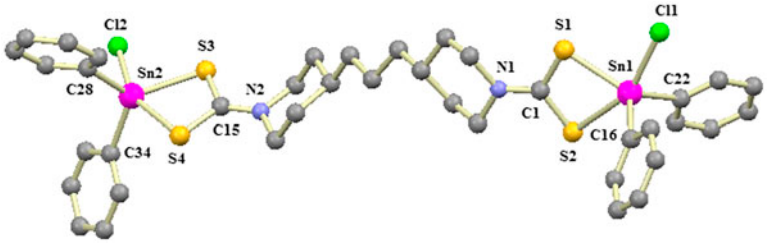

Figure 2. Molecular structure of **2**.

Table 1. Bond lengths (Å) and angles (°) of **1** and **2**.

Bond lengths (Å)			Bond angles (°)		
	$(n\text{-}Bu_2SnCl)_2L$ (**1**)	$(Ph_2SnCl)_2L$ (**2**)		$(n\text{-}Bu_2SnCl)_2L$ (**1**)	$(Ph_2SnCl)_2L$ (**2**)
Sn–Cl	2.4570(8)	2.462(3)	$Cl–Sn–S_{long}$	155.69(2)	154.50(10)
	2.470(7)/2.469(9)	2.473(3)	(β)	156.3(3)/156.0(4)	155.36(9)
$Sn–S_{short}$	2.4565(7)	2.471(3)	$C_{eq.}–Sn–C_{eq.}$	123.80(11)	129.1(3)
	2.5058(10)/2.4201(11)	2.462(3)	(α)	124.5(3)/122.7(3)	122.2(3)
$Sn–S_{long}$	2.7404(7)	2.655(3)	$Cl–Sn–S_{short}$	87.27(2)	85.09(10)
	2.736(11)/2.689(13)	2.693(3)		88.53(15)/85.0(2)	85.65(9)
$C–S_{short}$	1.750(3)	1.733(14)	$S_{short}–Sn–S_{long}$	69.12(2)	70.17(10)
	1.752(3)	1.734(11)		68.1(2)/70.9(3)	69.71(9)
$C–S_{long}$	1.708(3)	1.728(13)			
	1.727(12)/1.705(14)	1.740(11)			

Note: Two values: values for model A (occupancy factor 0.537(3), major values for model B (occupancy factor 0.463(3)), minor.

coordination of both 1,1-dithioate moieties of the ligand is asymmetric with $Sn–S_{short}$ [complex **1** = 2.4565(7), 2.4201(11) and complex **2** = 2.471(3), 2.462(3)] and $Sn–S_{long}$ [complex **1** = 2.7404(7), 2.689(13) and complex **2** = 2.655(3), 2.693(3)] bonds. The short Sn–S bond is associated with a long C–S bond length and vice versa. In both complexes, geometry around Sn can be characterized by τ value using equation $(\beta - \alpha)/60$ [24]. Here β and α are the largest of the basal angles around the Sn atom. The angle $\beta = \alpha = 180°$ correspond to a square-pyramidal with τ value zero and $\alpha = 120$ (τ is unity) match with a perfectly

trigonal-bipyramidal geometry. In **1**, the geometry around both tins is between trigonal-bipyramidal and square pyramidal with a τ value of 0.53. However, in **2** the geometry around one of the two tins is slightly biased towards square pyramidal (0.42 and 0.55). The chloride occupies one axial position while sulfur forming long Sn–S bond occupies the other one. However, being a part of a chelate sulfur is pseudoaxial, giving rise to an angle of around 155°.

In **3** and **4**, both the tin centers are coordinated asymmetrically to CS_2 and three organic groups (figures 3 and 4, table 2). However, the mode of coordination of ligand to both tins is slightly different {[(Sn1–S1a = 2.699(3), Sn1–S2b = 2.919(3) Å] and [Sn2–S3 = 2.4735 (10), Sn2–S4 = 2.9468(10) Å]} and the Δ(Sn–S) is 0.22 and 0.47 Å. These values are comparable with reported triorganotin(IV) dithiocarbamates [25]. In **3**, the geometry around Sn1 is distorted square pyramidal (0.24) and for Sn2 it is between the two (0.45). The long Sn–S bond again is on a pseudo-apical position, thus C–Sn–S_{long} angles are reduced to 151.34(15)° and 154.45(10)°.

Packing diagram of **1** suggests that a chain is mediated by H18B···Cl2 (2.795 Å) interactions (0.1 Å less than van der Waal's radii) with intermolecular Sn···Sn distance of 5.952 Å [figure 5(a)]. The chain is further strengthened by Cl1···H27C (2.830 Å) interactions. Neighboring chains are linked via Cl1 and H2A (2.907 Å) of piperidine to generate a supramolecular structure [figure 5(b)]. For **2**, intermolecular interactions (Å): C19···H3B 2.720,

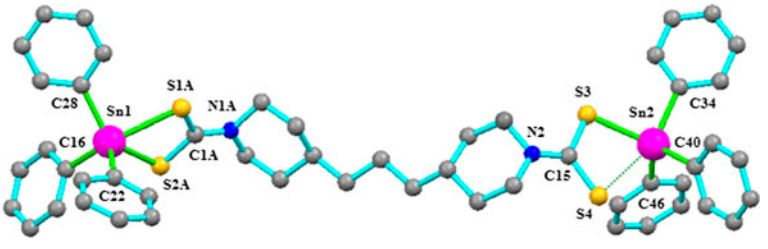

Figure 3. Ball and stick diagram of **3**.

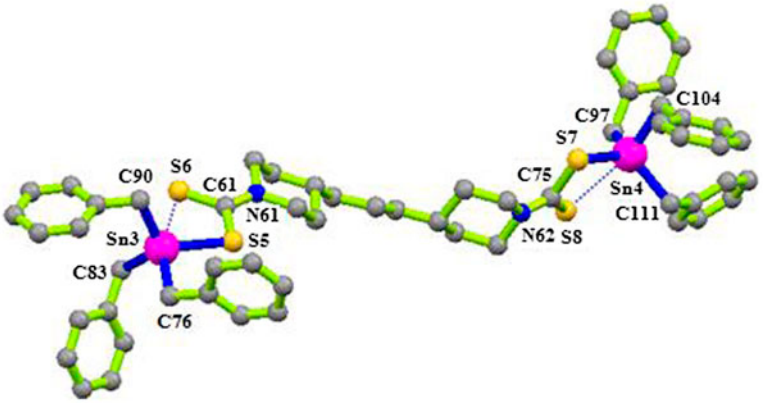

Figure 4. Ball and stick diagram of **4**.

Table 2. Bond lengths (Å) and angles (°) of **3** and **4**. For **4** the data are presented for molecule 1 [molecule 2].

Bond lengths (Å)			Bond angles (°)		
	$(Ph_3Sn)_2L$ (**3**)	$(Bz_3Sn)_2L$ (**4**)		$(Ph_3Sn)_2L$ (**3**)	$(Bz_3Sn)_2L$ (**4**)
$Sn–S_{short}$	2.507(4)	2.4730(11)	$C_{axial}–Sn–S_{long}$	151.34(15)	160.16
	2.4735(10)	[2.4730(12)]	(β)	152.07(13)	[159.07]
		2.4786(11)			160.02
		[2.4763(11)]			[159.77]
$Sn–S_{long}$	2.699(3)	2.932	$C_{eq.}–Sn–S_{short}$	136.51(17)	122.67(13)
	2.9468(10)	[2.949]	(α)	127.32(10)	[120.62(16)]
		2.963			115.95(14)
		[2.951]			[118.12(14)]
$C–S_{short}$	1.723(9)	1.764(5)	$C_{eq.}–Sn–C_{eq.}$	109.70(14)	115.0(2)
	1.705(9)	[1.764(4)]		109.98(15)	[115.3(2)]
		1.766(5)			116.80(19)
		[1.769(5)]			[116.51(19)]
$C–S_{long}$	1.742(4)	1.697(5)	$S_{short}–Sn–S_{long}$	68.14(9)	66.11
	1.701(4)	[1.688(5)]		65.34(3)	[65.85]
		1.699(5)			65.58
		[1.696(5)]			[65.68]

C31···H6A 2.667, C32···H6A 2.633, H7A···C28 2.766, C20···H14B 2.702, and C39···H26 2.709 Å [figure 6(a)] mediate a supramolecular structure which looks like parallel chains when viewed along the *a*-axis [figure 6(b)]. In **3**, C51···H33 2.799, H2A···C47 2.367, C48···H2A 2.615, C23···H35 2.794, H7B···H21 2.293, and C18···H4A 2.766 intramolecular

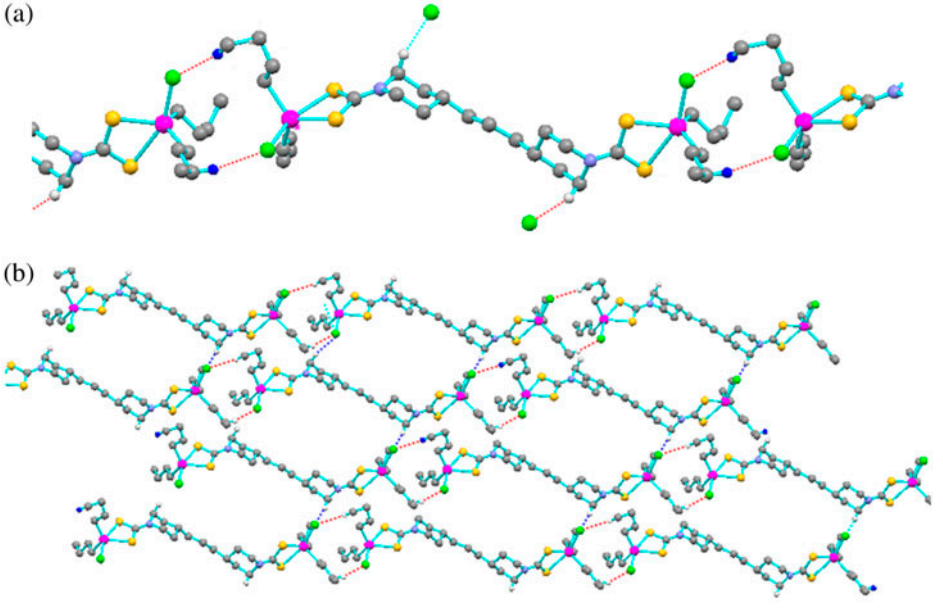

Figure 5. (a) H18B···Cl2 2.795 Å and Cl1···H27C 2.830 Å mediate a chain and (b) neighboring chains connected via Cl1···H2A-piperidine 2.907 Å to form supramolecule **1**.

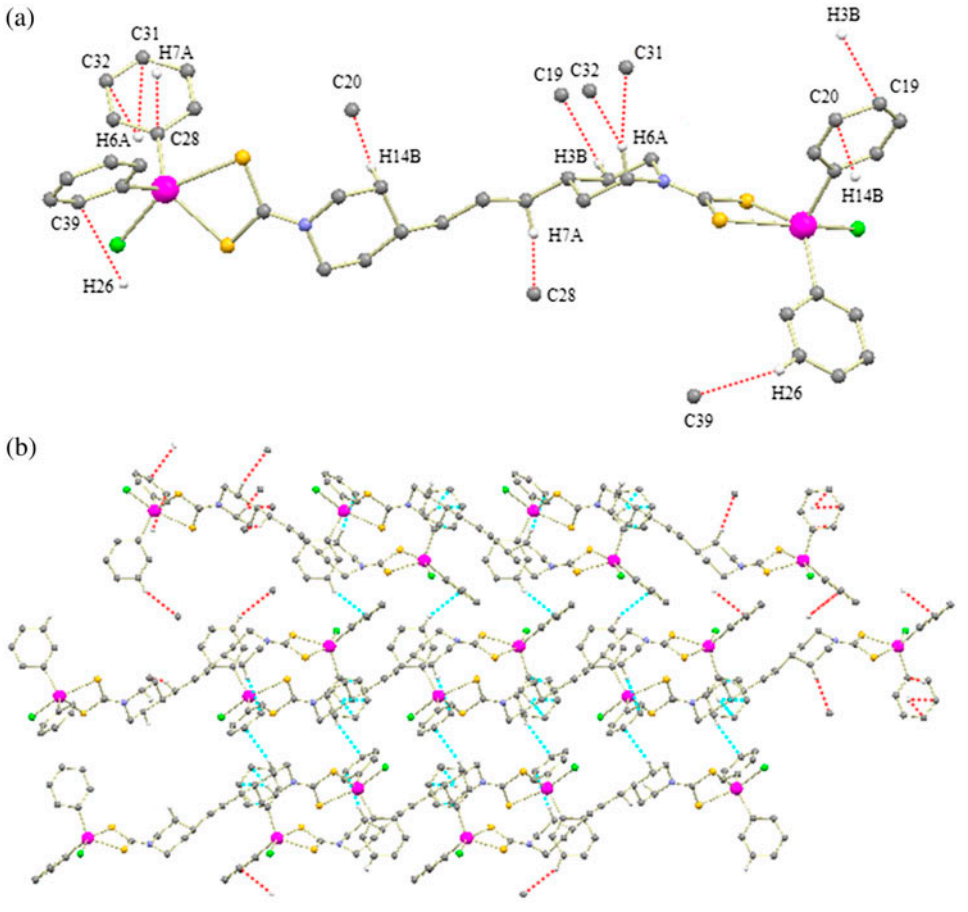

Figure 6. (a) Structure showing types of intermolecular interactions 0.1 Å less than the van der Waal's radii of the connected atoms; (b) supramolecular structure illustrating parallel chains along the *a*-axis for **2**.

interactions make a supramolecular structure [figure 7(a) and (b)]. In **4**, intermolecular association via C91···H65B (2.766 Å) and C61···H62B (2.764 Å) interactions form a chain-like structure (figure 8).

3. Biological activities

3.1. *Antileishmanial activity and docking analysis*

The ligand and **1–4** were screened against the pathogenic *Leishmania major* using Amphotericin B (0.342 μg mL^{-1}) as a standard drug (figure 9). All the studied organotin(IV) derivatives were more active than the corresponding free ligand, authenticating the dynamic role of Sn in the antileishmanial activity. The activity reduces in the order: $(Bz_3Sn)_2L$ >> $(Bu_2SnCl)_2L$ > $(Ph_3Sn)_2L$ > $(Ph_2SnCl)_2L$. According to our previous findings [15], the antileishmanial activity is governed by planarity, lipophilicity, and low-molecular weight.

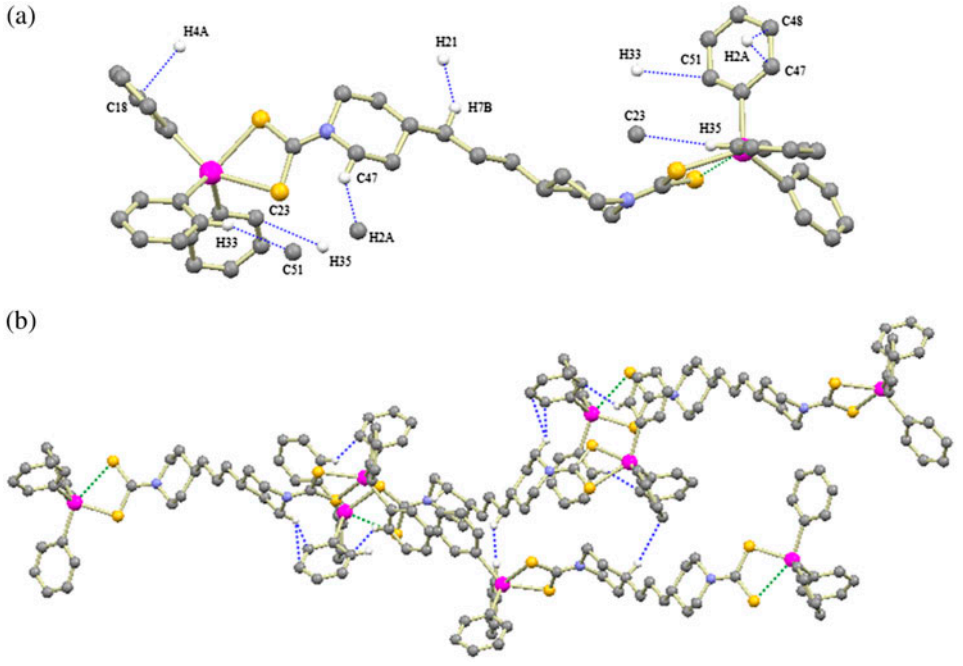

Figure 7. (a) Interacting atoms that form supramolecular structure; (b) supramolecular structure of **3**.

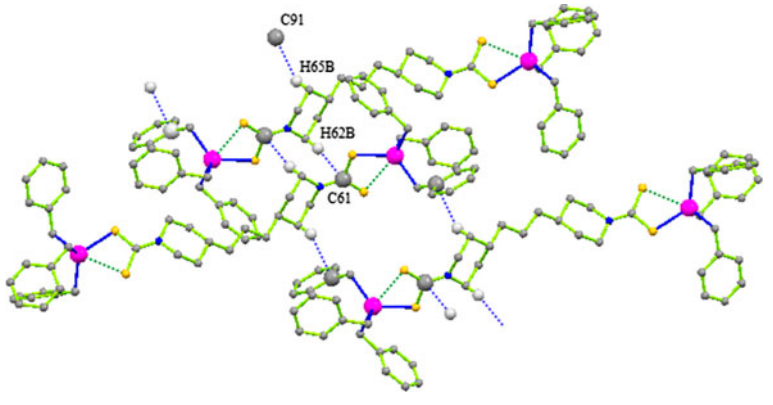

Figure 8. Supramolecular molecular chain of **4** formed by C91···H65B (2.766 Å) and C61···H62B (2.764 Å) interactions.

However, the high activity of $(Bz_3Sn)_2L$ points to another factor, the geometry around Sn. Four-coordinate $[(Bz_3Sn)_2L)]$ was more active than five-coordinate ones. Although all the compounds have the potential to be used as drugs, $(Bz_3Sn)_2L$ is a leading candidate in this connection due to high activity and reasonable cytotoxicity LD_{50} value (11.921 μg mL^{-1}). These compounds, especially the last one, may emerge as a novel class of antileishmanial drugs alone or in combination with other drugs.

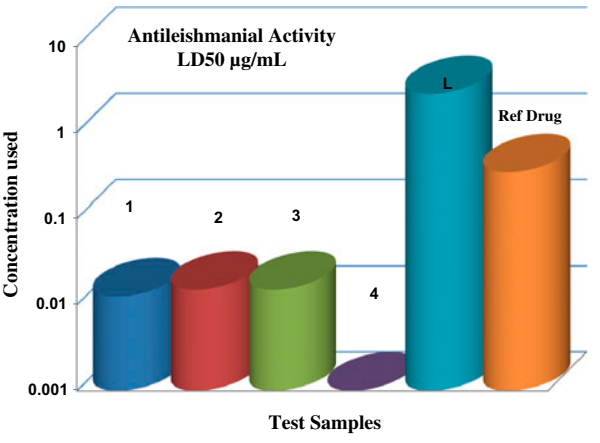

Figure 9. Comparative antileishmanial activity of ligand, complexes **1–4** and reference drug.

Figures 10–14 represent the preferred binding orientation of **1–4** with TryS in their lowest binding energy. All of the compounds preferred to bind with chain A of the enzyme as depicted in figures 10–14. Binding energy obtained after docking was −13.14, −11.46, −11.13, and −10.07 kcal M^{-1} for $(Bz_3Sn)_2L$, $(Bu_2SnCl)_2L$, $(Ph_3Sn)_2L$, and $(Ph_2SnCl)_2L$, respectively. Binding energy order of all of the compounds is in agreement with experimental antileishmanial activity which supports the accuracy of both the experimental and the docking analysis. The lowest binding energy refers to the most stable complexation between enzyme and complex. In our case, $(Bz_3Sn)_2L$ got the lowest binding energy with enzyme TryS, which suggests $(Bz_3Sn)_2L$ binds with greater strength with TryS compared with other compounds. This strong binding would ultimately inhibit some functions of enzyme as the binding site is already in use for $(Bz_3Sn)_2L$. In our experimental studies of antileishmanial

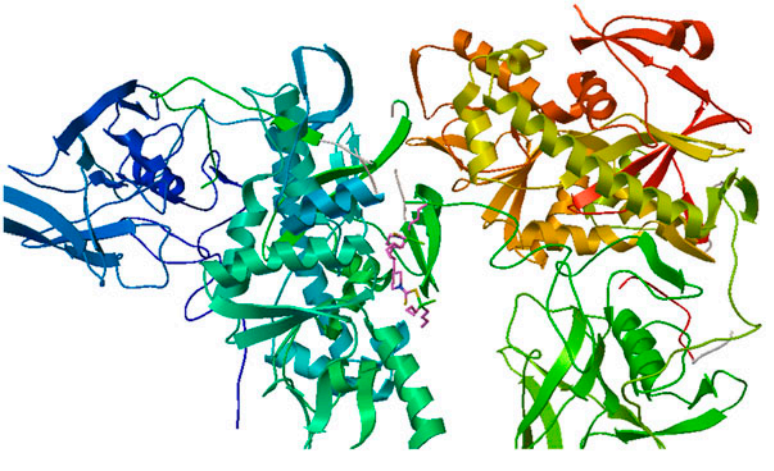

Figure 10. Molecular docking of **1** with TryS (2VOB) showing the preferred binding orientation with Chain A of TryS.

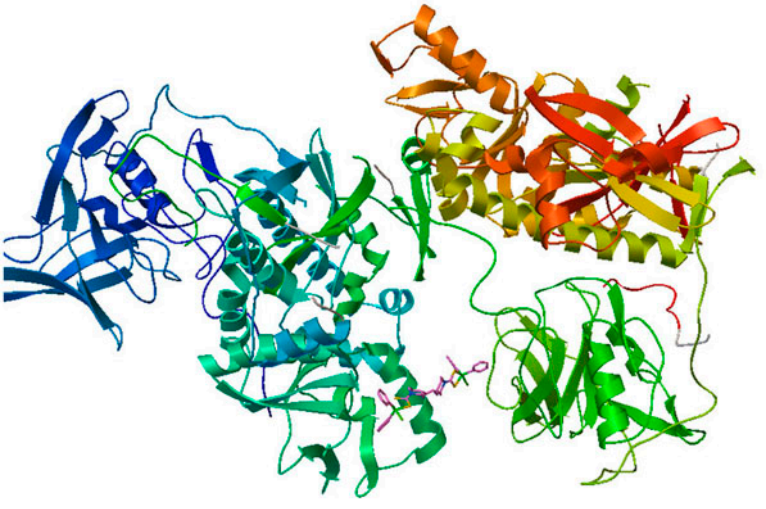

Figure 11. Molecular docking of **2** with TryS (2VOB) showing the preferred binding orientation with Chain A of TryS.

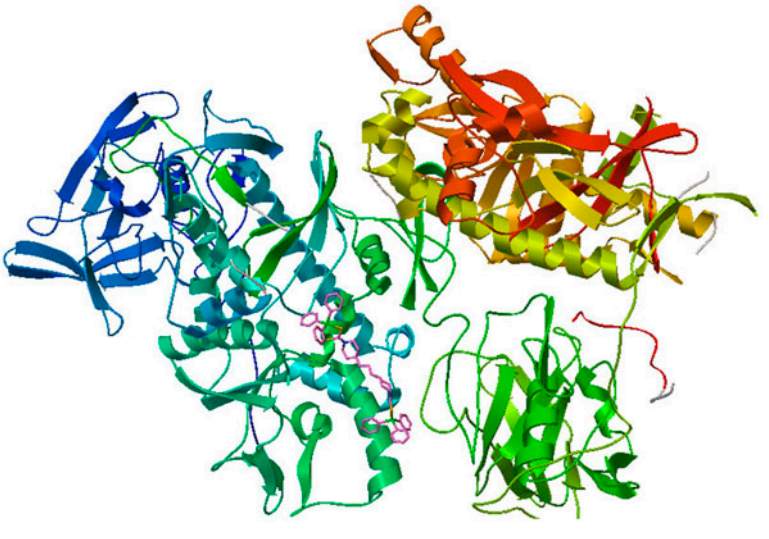

Figure 12. Molecular docking of **3** with TryS (2VOB) showing the preferred binding orientation with Chain A of TryS.

activity, $(Bz_3Sn)_2L$ is better than other inhibitors which is explainable on the basis of its lowest binding energy with TryS during docking analysis. In order to predict the preferred inhibition mechanism of $(Bz_3Sn)_2L$ with TryS, surface-to-surface interactions were explored as shown in figure 14. Benzyl groups are surrounding the cavity close to the spermidine binding cleft, and are well fitted within the cavity thereby blocking this enzyme site for normal functions. Residues surrounding the cavity GLU405, 407 and 408 are interacting with

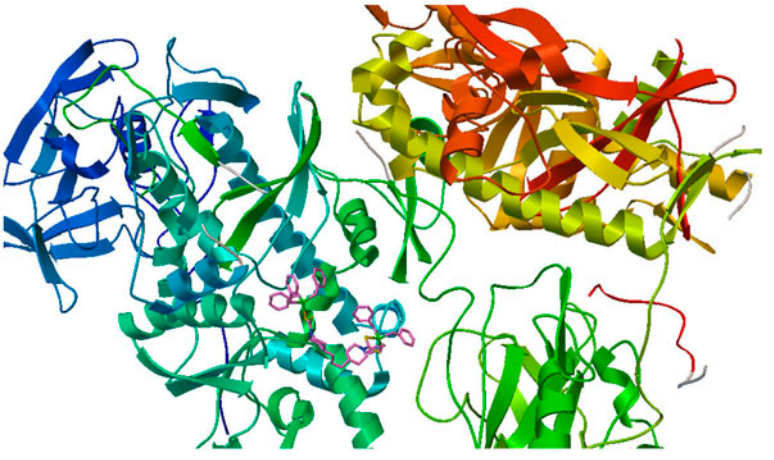

Figure 13. Molecular docking of **4** with TryS (2VOB) showing the preferred binding orientation with Chain A of TryS.

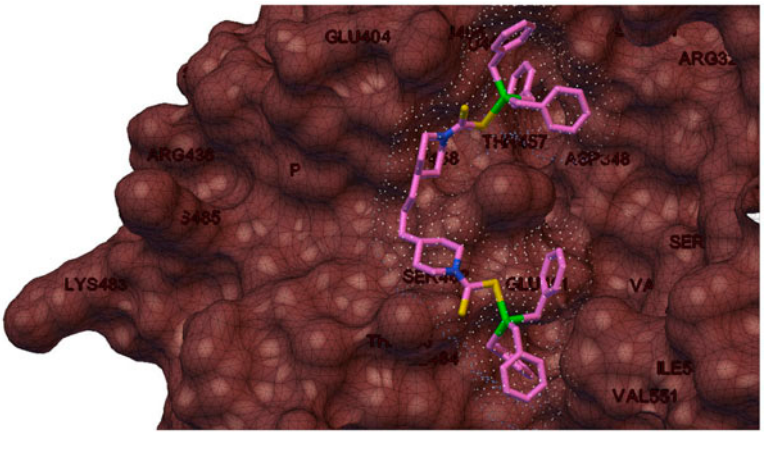

Figure 14. Interaction of molecular surface of **4** with surface of Chain A of TryS showing the close up encounters of inhibitor with spermidine binding domain of the enzyme. White dots around the compound represent its surface.

phenyl groups attached to $(Bz_3Sn)_2L$. Other parts of $(Bz_3Sn)_2L$ are surrounded with residues SER462, GLU461, TRP458, THR457, THR465, ASP348, ILE464, and ASP466 attached to the A chain of TryS.

3.2. *Cytotoxicity assay*

The cytotoxicities of the ligand-salt and **1–4** were studied by brine shrimp method lethality (table 3). The activity of the compound is given in table 3 using Doxorubicin as a reference drug. The LD_{50} ($\mu g\,mL^{-1}$) value of a tested compound is calculated statistically by SPSS version 21 software. All the complexes are more active than the ligand, comparable with

Table 3. LD_{50} ($\mu g\,mL^{-1}$) values for the ligand and **1–4**.

Compound	LD_{50}
$(Bu_2SnCl)_2L$ (**1**)	5.22
$(Ph_2SnCl)_2L$ (**2**)	0.415
$(Ph_3Sn)_2L$ (**3**)	16.543
$(Bn_3Sn)_2L$ (**4**)	11.921
L	543.17
Doxorubicin	7.23

earlier report [26]. The comparative study showed that diorgantin(IV) complexes were more toxic than triorganotins.

4. Conclusion

New homobimetallic organotin(IV) dithiocarbamates have been synthesized and characterized by X-ray single crystal analysis, FT-IR, and multinuclear NMR spectroscopy. The appearance of new vibrations for Sn–S (365–375 cm^{-1}) and Sn–C (440–450 cm^{-1}) which was absent in the free ligand salt suggest formation of **1–4**. A single peak at 950–970 cm^{-1} for ν(C–S) was suggestive of bidentate coordination of ligand, further supported by X-ray single crystal analysis, which confirmed anisobidentate mode of 1,1-dithiolate moiety with shorter and longer Sn–S bonds. Molecules in the solid state are linked via noncovalent C···H and Cl···H interactions to generate supramolecular architectures. The ^1H and ^{13}C NMR have suggested that Sn (**1–3**) maintain their solid state five-coordination in solution, however, coordination switches from five to four in solution for **4**. The ligands and their complexes have good antileishmanial activity. **1–4** supersede the ligand in activity, thus confirming the vital role of Sn in the antileishmanial action. The antileishmanial activities of **1–4** are well above the standard drug. The docking study has proposed that the high activity of **4** was due to its lowest binging energy with enzyme TryS.

5. Experimental

5.1. *Chemicals and instrumentation*

All the chemicals used for synthetic work were of high purity. Tin powder, benzyl chloride, ethyl acetate, glacial acetic acid, 4,4-trimethylene-dipiperidine (precursor), and organotin salt (R_2SnCl_2 and R_3SnCl) were purchased from Fluka and Sigma-Aldrich chemical companies. Tribenzyltin chloride was prepared by the reported method [27]. CS_2 was obtained from Reidel-de-Haen. Analytical grade solvents (ethanol, DMSO methanol, DMF, chloroform, and dichloromethane) were purchased from E-Merck and Fluka.

The melting points were recorded on an electrothermal melting point apparatus, model MP-D Mitamura Rieken Kogyo (Japan) by using capillary tubes and are uncorrected. The FT-IR spectra from 4000 to 200 cm^{-1} were taken in capillary tubes using Perkin Elmer spectrum 1000 (USA). Multinuclear NMR (^1H and ^{13}C) spectra were recorded on a Bruker

Avance 300 MHz NMR instrument using $CDCl_3$ as an internal reference. Chemical shifts (δ) and coupling constants (J) are given in ppm and Hz, respectively. The multiplicities of signals in ^1H NMR are given with chemical shifts.

5.2. *X-ray single crystal analysis*

Suitable single crystals of **1–4** were selected and mounted on a Microstar diffractometer. During data collection, the crystal was kept at 100 K. Using Olex2 [28], the structure was solved with the XS [29] structure solution program using Direct Methods and refined with the XL [29] refinement package using Least Squares minimization.

5.3. *Synthesis*

5.3.1. Synthesis of ligand salt. About 2 gram (9.5 mM) of 4,4′-trimethylenedipiperidine was dissolved in methanol, followed by the addition of 0.76 g (19 mM) of aqueous NaOH, and the mixture was stirred at room temperature for 2 h. Afterwards, 1.14 mL (19 mM) CS_2 dissolved in methanol was added dropwise at 0 °C and stirred for 5 h. The resultant solution was evaporated to get a yellowish solid (scheme 1). Yield 85%. M.p. 223–224 °C. IR (KBr, cm^{-1}) v: 1469 (N–CSS), 961 (SCS). ^1H NMR (300 MHz, $CDCl_3$): δ = 5.74 (d, J = 12 Hz, 4H, 2-H_e), 2.77 (t, J = 12 Hz 4H, 2-Ha), 1.56 (d, J = 12 Hz, 4H, 3-H_e), 1.44 (q, J = 7.7 Hz, 4H, 5-H), 1.43–0.90 (m, 8H, 3-H_a, 4-H, 6-H) ppm. ^{13}C NMR (75 MHz, $CDCl_3$): δ = 213.0 (C-1), 50.0 (C-2), 32.7 (C-3), 36.7 (C-4), 36.0 (C-5), 23.8 (C-6) ppm.

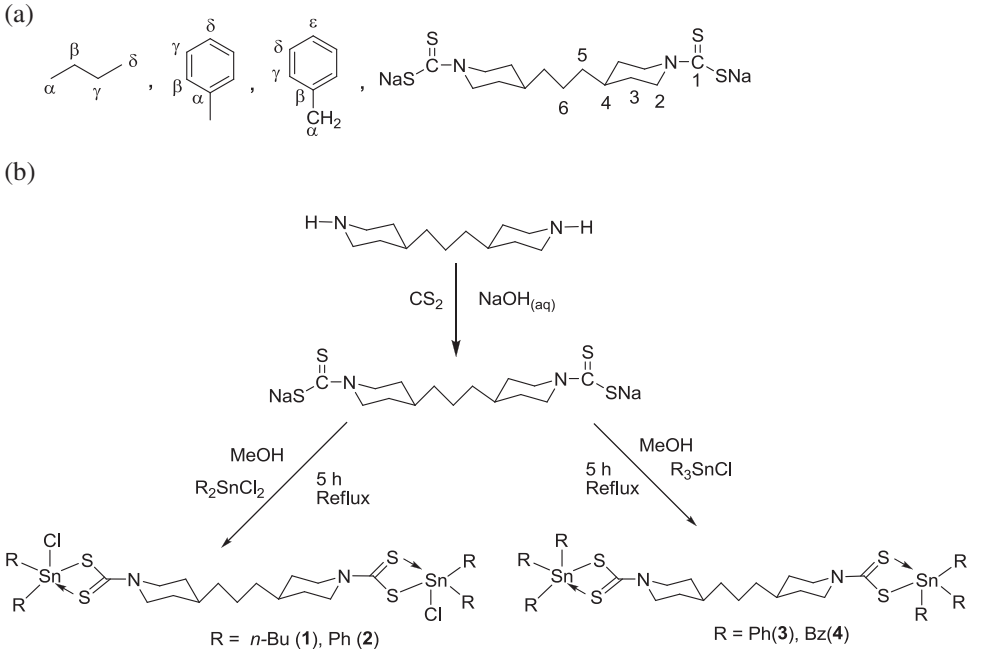

Scheme 1. (a) Numbering scheme of the ligand salt and Sn attached organic groups and (b) synthesis of ligand salt and its organotin(IV) derivatives (**1–4**).

5.3.2. Synthesis of chloroorganotin(IV) derivatives (1 and 2). Diphenyltin(IV) dichloride 0.01 M (3.43 g) and dibutyltin(IV) dichloride 0.01 M (3.03 g) were dissolved in toluene and ligand 0.005 M (2.03 g) was dissolved in methanol; both solvents were mixed and refluxed for 4 h with continuous stirring. The salt was allowed to settle and was removed by filtration. The filtrate was rotary evaporated to obtain the product (scheme 1). The resultant product was recrystallized in a mixture of CH_2Cl_2 and n-C_6H_{12} in 3 : 1 ratio.

($Bu_2SnCl)_2L$ (1): Yield 87%. Colorless crystals. M.p. 96 °C. IR (KBr, cm^{-1}) ν: 1508 (N–CSS), 971 (S–CS), 447 (Sn–C), 371 (Sn–S), 303 (Sn–Cl)); ^{1}H NMR (300 MHz, $CDCl_3$): δ = 4.72 (d, J = 12 Hz, 4H, 2-H_e), 3.14 (t, J = 12 Hz, 4H, 2-Ha), 1.88–1.253 m (4H, 3-H_e; 4H, 5-H; 8H, 3-H_a, 4-H, 6-H; α, β, γ-H), 0.94 (t, J = 7.5 Hz, δ-H) ppm. ^{13}C NMR (75 MHz, $CDCl_3$): δ = 195.2 (CSS), 52.7(C-2,2), 35.8 (C-3,3), 35.4 (C-4), 34.5 (C-5) 23.7 (C-6), 29.1 (C-α, J = 558 Hz, 125°), 27.9 (C-β, J = 33 Hz), 26.3, (C-γ, J = 96.7 Hz), 17.5 (δ).

($Ph_2SnCl)_2L$ (2): Yield 91%. Colorless crystals. M.p. 156 °C; IR (KBr, cm^{-1}) ν: 1505 (N–CSS), 968 (S–CS), 445 (Sn–C), 371 (Sn–S), 310 (Sn–Cl)); ^{1}H NMR (300 MHz, $CDCl_3$): δ = 4.70 (d, J = 12 Hz, 4H, 2-H_e), 3.18 (t, J = 12 Hz, 4H, 2-Ha), 1.87 (d, J = 12 Hz, 4H, 3-H_e), 1.44 (q, J = 7.7 Hz, 4H, 5-H), 1.29–1.37 (m, 8H, 3-H_a, 4-H, 6-H), 8.07 (d, 8H, *ipso*-H, ^3J (^{119}Sn, ^{1}H) = 49.5), 7.28–7.56 (m, 12H, γ-H, δ-H) ppm. ^{13}C NMR (75 MHz, $CDCl_3$): δ = 194.0 (C-1), 53.3 (C-2), 31.8 (C-3), 35.6 (C-4), 34.2 (C-5) 23.6 (C-6), 142.0 (α, J = 578 Hz), 137.6 (C-β, J = 64 Hz), 130.2 (γ, J = 18 Hz), 128.2 (δ, J = 88 Hz) ppm.

5.3.3. Synthesis of triphenyl- and tribenzyltin(IV) derivatives (3 and 4). The metal salt of triphenyltin(IV) chloride 0.01 M (3.85 g) and tribenzyltin(IV) chloride 0.01 M (4.27 g) was separately dissolved in methanol, followed by addition of 0.005 M (2.03 g) of the ligand salt to each. The reaction mixture was stirred for 5 h at room temperature. The resultant product was insoluble in methanol and was filtered out (scheme 1). The product was recrystallized in the mixture of CH_2Cl_2 and CH_3OH in 3 : 1 ratio.

($Ph_3Sn)_2L$ (3): Yield 89%. Colorless crystals. M.p. 170 °C; IR (KBr, cm^{-1}) ν: 1488 (N–CSS), 960 (SCS), 449 (Sn–C), 373 (Sn–S); ^{1}H NMR (300 MHz, $CDCl_3$: δ = 4.99 (d, J = 13 Hz, 4H, 2-H_e), 3.14 (t, J = 11 Hz 4H, 2-Ha), 1.79 (d, J = 11 Hz, 4H, 3-H_e), 1.48 (q, J = 7.7 Hz, 4H, 5-H), 1.28–1.35 (m, 8H, 3-H_a, 4-H, 6-H), 7.857 (d, 12H, *ipso*-H, ^3J (^{119}Sn, ^{1}H) = 49.2), 7.46–7.28 (m, 18H, γ-H, δ-H) ppm. ^{13}C NMR (75 MHz, $CDCl_3$): δ = 194.6 (CSS), 53.4 (C-2,2), 35.9 (C-3,3), 142.7 (C-α, J = 600.7 Hz, 129°), 136.8 (C-β, J = 45.7 Hz), 128.1 (C-γ, J = 60.7 Hz), 129.12 (C-δ J = 12.75 Hz) ppm.

($Bz_3Sn)_2L$ (4): Yield 93%. Colorless crystals. M.p. 125 °C; IR (KBr, cm^{-1}) ν: 1488 (N–CSS), 961 (S–CS), 446 (Sn–C), 369 (Sn–S). δ = 5.00 (d, J = 13 Hz, 4H, 2-H_e), 3.07 (t, J = 11 Hz, 4H, 2-Ha), 1.70 (d, J = 12 Hz, 4H, 3-H_e), 1.43 (q, J = 7.7 Hz, 4H, 5-H), 1.26–1.34 (m, 8H, 3-H_a, 4-H, 6-H), 7.857 (s, 6H, *ipso*-H, ^2J (^{119}Sn, ^{1}H) = 49 Hz, 107°), 6.81–7.28 (m, 30H γ, δ, Ɛ-H) ppm. ^{13}C NMR (75 MHz, $CDCl_3$): δ = 195.6 (CSS), 53.1 (C-2,2), 36.0 (C-3,3), 26.8 (α, J = 302 Hz, 103°), 140.1 (β, J = 40.5 Hz), 127.9 (γ, J = 30 Hz), 124.2 (δ J = 21.75 Hz), 128.5 (Ɛ, J = 18 Hz) ppm.

5.4. *Antileishmanial assay and docking analysis*

Pre-established *Leishmania tropica* (kwh 23) culture was incubated at 24 °C for 6–7 days in 199 medium containing 10% Fetal Bovine Serum (purchased from PAA Lab, Gmbh). For

in vitro antileishmanial activity, stock solution of the samples was prepared by dissolving 6 mg in 600 µL of DMSO to get 10,000 ppm as described previously [30] with a slight modification. The stock solutions were serially diluted. The first row of the 96-well plate contained 196 µL of 199 medium containing about 100 promastigotes and the remaining well contained 180 µL of 199 medium. About 4 µL of the test sample were added into each well of the first row of the plate to get a total concentration of 200 ppm, mixed and serially diluted to keep the final volume 180 µL; 20 µL were discarded from the last well. The concentration of DMSO was kept <5% which has no toxic effect on leishmania. For negative and positive control DMSO and DMSO-containing drug, Amphotericin B was used, respectively, and serially diluted. The microtitre plates were then incubated for 72 h at 24 °C. The experiment was performed in triplicate. After 72 h, about 15 µL of culture were then transferred to an improved neobar counting chamber and live promastigote were counted under a light microscope. To calculate IC_{50} value, the data were subjected to Probit regression Analysis, SPSS version 21 software.

Docking studies were carried out using Autodock (Version 4.2) docking software [31]. Structure of TryS (2VOB) was taken from the protein data bank [32]. All bound waters and cofactors were removed from the protein manually, Geisteger charges were computed, polar hydrogens were added subsequently, and the AutoDock atom types were defined using AUTODOCK Tools, graphical user interface of AUTODOCK supplied by MGL Tools. Three-dimensional STRUCTURE of complexes wase obtained from crystallographic information file. The default root, rotatable bonds, and torsions of the ligand were set by TORSDOF utility in AutoDock Tools.

Docking was done by implementing Lamarckian Genetic Algorithm (LGA) which is considered one of the best docking methods available in AutoDock. LGA has enhanced performance compared to simulated annealing or the simple genetic algorithm among the other search algorithms available in AutoDock4 for ligand conformational searching [33]. The algorithm uses a five-term force field-based function derived from the AMBER force field, and that comprises a Lennard–Jones dispersion term, a directional hydrogen bonding term, a Coulombic electrostatic potential, an entropic term, and an intermolecular pairwise desolvation term [34]. The scaling factor for each of these five terms is empirically calibrated from a set of 30 structurally known protein–ligand complexes. The ligand translation, rotation, and internal torsions are defined as state variables, and each gene represents a state variable. LGA adds local minimization to the genetic algorithm, enabling modification of the gene population [35].

5.5. *Cytotoxicity assay*

Brine shrimp cytotoxicity assay was performed by a minor modification in the previously reported method [36]. Different reagents and material required for the experiments were: tray for hatching eggs, lamp for larvae attraction, test sample, sea salt (40 g L^{-1} in distilled water, maintaining a pH of 7.4), micro pipette, and DMSO.

Test samples (6 mg) were weighed and dissolved in 600 µL of DMSO to get a stock solution of 10,000 ppm. Different dilutions ranging from 2 to 1000 ppm were prepared in separate vials. A total of 20 shrimps were transferred into each vial through a micro pipette. The volume of the vials was adjusted by means of sea salt water up to 5 mL. The cytotoxicity experiment was performed in triplicate at standard laboratory condition 25 ± 2 °C. The vials were then kept for 24 h. Positive and negative controls were maintained containing

DMSO plus drug Doxorubicin and DMSO plus sea salt water, respectively. After 24 h the data obtained were then statistically analyzed by Probit regression analysis SPSS version 21 software to get IC_{50} value.

Supplementary material

Single crystal X-ray diffraction data for the structural analysis have been deposited with the Cambridge Crystallographic Data Center, CCDC Nos. 975987 (**1**), 975988 (**2**), 975990 (**3**), and 975989 (**4**). The copy of this information may be obtained free of charge from the Director, CCDC, 12 Union Road, Cambridge CBZ 1EZ, UK (Fax:+44 1223 33,033; E-mail: deposit@ccdc.cam.ac.uk or www: http://www.ccdc.cam.ac.uk).

Funding

We acknowledge the financial support of Higher Education Commission of Pakistan and Quaid-i-Azam University, Islamabad, Pakistan.

References

[1] J.R. Brown, M. Hooper. *Critical Reports on Applied Chemistry: Chemotherapy of Tropical Diseases, Trypanosomiasis and Leishmaniasis*, Vol. 21, p. 72, John Wiley, Chichester (1987).
[2] P.L. Olliaro, A.D.M. Bryceson. *Parasitol. Today*, **9**, 323 (1993).
[3] P. Minodier, P. Parola. *Travel Med. Infect. Dis.*, **5**, 150 (2007).
[4] K.E. Kinnamon. *Antimicrob. Agents Chemother.*, **15**, 157 (1979).
[5] G. Lowe, A.S. Droz, T. Vilaivan, G.W. Weaver. *J. Med. Chem.*, **42**, 999 (1999).
[6] N. Mbongo, P.M. Loiseau, F. Lawrence, C. Bories, D.G. Craciunescu, M. Robert-Gero. *Parasitol. Res.*, **83**, 515 (1997).
[7] M. Navarro, C. Hernandez, I. Colmenares, P. Hernandez. *J. Inorg. Biochem.*, **101**, 111 (2007).
[8] S.P. Fricker, R.M. Mosi, B.R. Cameron, I. Baird. *J. Inorg. Biochem.*, **102**, 1839 (2008).
[9] U. Salma, Imtiaz-ud-Din, M. Mazhar, K.M. Khan. *Med. Chem.*, **543**, 5 (2009).
[10] U. Salma, M. Mazhar, Imtiaz-ud-Din, S. Ali, K.M. Khan. *J. Enzyme Inhib. Med. Chem.*, **24**, 413 (2009).
[11] D.B. Kitchen, H. Decornez, J.R. Furr, J. Bajorath. *Nat. Rev. Drug Discov.*, **3**, 935 (2004).
[12] S.L. Croft, G.H. Coombs. *Trends Parasitol.*, **19**, 502 (2003).
[13] S.L. Oza, S. Chen, S. Wyllie, J.K. Coward, A.H. Fairlamb. *FEBS J.*, **275**, 5408 (2008).
[14] S.K. Venkatesan, P. Saudagar, V.K. Dubey. *J. Proteins Proteomics*, **2**, 41 (2011).
[15] S. Shujah, Zia-ur-Rehman, N. Muhammad, S. Ali, N. Khalid, M.N. Tahir. *J. Organomet. Chem.*, **696**, 2772 (2011).
[16] S. Shujah, Zia-ur-Rehman, N. Muhammad, A. Shah, S. Ali, N. Khalid, A. Meetsma. *J. Organomet. Chem.*, **741**, 59 (2013).
[17] H.D. Yin, S.C. Xue. *Appl. Organomet. Chem.*, **20**, 283 (2006).
[18] A. Mohammad, C. Varshney, S.A.A. Nami. *Spectrochim. Acta, Part A*, **73**, 20 (2009).
[19] L. Ronconi, C. Maccato, D. Barreca, R. Saini, M. Zancato, D. Fregona. *Polyhedron*, **24**, 521 (2005).
[20] F. Bonati, R. Ugo. *J. Organomet. Chem.*, **10**, 257 (1967).
[21] M. Nadvornik, J. Holecek, K. Handlir. *J. Organomet. Chem.*, **275**, 43 (1984).
[22] T.P. Lockhart, F. Davidson. *Organometallics*, **6**, 2471 (1987).
[23] T.S.B. Baul, S. Dhar, S.M. Pyke, E.R.T. Tiekink, E. Rivarola, R. Butcher, F.E. Smith. *J. Organomet. Chem.*, **633**, 7 (2001).
[24] A.W. Addison, T.N. Rao, J. Reedijk, J. Van Rijn, G.C. Verschoor. *J. Chem. Soc., Dalton Trans.*, 1349 (1984).
[25] Zia-ur-Rehman, A. Shah, N. Muhammad, S. Ali, R. Qureshi, I.S. Butler. *Eur. J. Med. Chem.*, **44**, 3986 (2009).
[26] S. Jabbar, I. Shahzadi, R. Rehman, H. Iqbal, Qurat-Ul-Ain, A. Jamil, R. Kousar, S. Ali, S. Shahzadi, M. Aziz. *J. Coord. Chem.*, **65**, 572 (2012).
[27] K. Sisido, Y. Takeda, Z. Kingawa. *J. Am. Chem. Soc.*, **83**, 538 (1961).
[28] O.V. Dolomanov, L.J. Bourhis, R.J. Gildea, J.A.K. Howard, H. Puschmann. *J. Appl. Cryst.*, **42**, 339 (2009).
[29] G.M. Sheldrick. *Acta Cryst.*, **A64**, 112 (2008).

[30] S. Nabi, N. Ahmed, M.J. Khan, Z. Bazai, M. Yasinzai, Y.M.S.A. Al-Kahraman. *World Appl. Sci. J.*, **19**, 1495 (2012).
[31] G.M. Morris, R. Huey, W. Lindstrom, M.F. Sanner, R.K. Belew, D.S. Goodsell, A.J. Olson. *J. Comput. Chem.*, **30**, 2785 (2009).
[32] H.R. Drew, R.M. Wing, T. Takano, C. Broka, S. Tanaka, K. Itakura, R.E. Dickerson. *Proc. Natl. Acad. Sci.*, **78**, 2179 (1981).
[33] R. Huey, G.M. Morris, A.J. Olson, D.S. Goodsell. *J. Comput. Chem.*, **28**, 1145 (2007).
[34] S. Betzi, C. Eydoux, C. Bussetta, M. Blemont, P. Leyssen, C. Debarnot, M. Ben-Rahou, J. Haiech, M. Hibert, F. Gueritte. *Antiviral Res.*, **84**, 48 (2009).
[35] S.K. Venkatesan, A.K. Shukla, V.K. Dubey. *J. Comput. Chem.*, **31**, 2463 (2010).
[36] A. Rehman, M.I. Choudhary, W.J. Thomsen. *Bioassay Techniques for Drug Development*, Harwood Academic Publishers, Amsterdam (2001).